

SIMULATION STUDIES ON GAX BASED KALINA CYCLE FOR BOTH POWER AND COOLING APPLICATIONS

C.P. Jawahar¹, R. Saravanan^{1*}, Joan Carles Bruno² and Alberto Coronas²

¹ Anna University, R & AC Lab, Dept. of Mechanical Engineering,
Sardar Patel Road, Guindy, Chennai – 600025, (India)

²Universitat Rovira i Virgili, CREVER-Group of Applied Thermal Engineering,
Avda. Paisos Catalans, 26, 43007 – Tarragona (Spain)

Abstract

A detailed parametric analysis is carried out on both simple and GAX based combined power and cooling cycle. The effect of various parameters such as heat source temperature, refrigeration temperature, sink temperature, split ratio (refrigerant flow ration between power and cooling systems), spilt factor (solution flow ration between absorber and GAX heat exchanger) on the performance of the cycle is studied. The results of the analysis shows that using the GAX heat exchanger about 20 % of internal heat is recovered within the cycle. The optimum spilt ratio is 0.8-0.9 and flow ratio is 0.5:0.5. The maximum combined thermal efficiency of 35-45 % and coefficient of performance of about 0.35 is attained at the optimum conditions.

Keywords

Absorption cooling systems, Power cycle, GAX, Kalina, COP, Thermal Efficiency

Introduction

In recent years, the concept of combined power and cooling cycles using ammonia-water as the working fluid have gained much attention [1]. The idea of utilizing a binary mixture such as ammonia-water was first proposed by Kalina, in the bottoming cycle of a combined power plant [2]. Subsequently, several researchers attempted to use ammonia-water in power cycle applications [3-5]. A combined power and cooling cycle originally proposed by Xu et al [6] showed that the cycle could achieve high thermal efficiency for a heat source temperature of about 400 K. Lu and Goswami [7] developed a combined power and refrigeration cycle and emphasized on the refrigeration part of the total output at low refrigeration temperatures. The performance of the combined cycle was determined at a wide range of low refrigeration temperatures and for a heat source temperature of 360K. A refrigeration temperature as low as 205K was achieved. At a refrigeration temperature of 245K, the first and second law efficiency reached a maximum of 17.4% and 63.7% respectively. A theoretical and experimental investigation of an ammonia-water power and refrigeration cycle has been done by Tamm et al [8]. The parametric analysis carried out revealed the potential for the cycle to be optimized for first and second law efficiency as well as power and cooling output. The thermal efficiency, power and the cooling output decreases by 20.6%, 11.8% and 37.7% respectively when the real losses are considered in the analysis. The experimental studies demonstrated the feasibility of a combined power and cooling cycle. The agreement between the theoretical and experimental results was found to be close. Zheng et al [9] proposed a combined power and cooling cycle based on the Kalina cycle, in which the flash tank or separator in Kalina cycle was replaced by a rectifier, to enhance the separation process and to obtain an additional higher purity stream of

Corresponding author: Tel: 91-44-22357578, Fax: 91-44-22353637

Email: rsaravanan@annauniv.edu

ammonia for cooling. The overall thermal efficiency and the exergy efficiency of the cycle were found to be 24.2% and 37.3% respectively. Martin and Goswami [10] evaluated the effectiveness of cooling production of the cycle by introducing a new parameter termed as effective COP. By using the effective COP as an objective function, the gain in the amount of cooling was optimized. Compared to the other work-driven cooling cycles, the maximum effective COP of the combined cycle was found to be nearly 1.1. Liu and Zhang [11] suggested a novel ammonia-water for the cogeneration of power and refrigeration driven by waste heat or flue gas from the turbine. The performance of the cycle was evaluated by exergy efficiency and found to be 58% for the base case studied. Compared with the conventional separate system of power generation and refrigeration, the cogeneration unit had nearly 18% reduction in energy consumption. Zhang and Lior [12] investigated three different configurations namely; parallel, series and compound cogeneration cycle configurations for the integration of refrigeration and power generation systems with a single heat source, using ammonia-water as the working fluid. In the configurations analyzed, the energy and exergy efficiencies were found to be 26 to 28% and 55 to 60% respectively, at a heat input temperature of 450°C. A combined refrigeration and power cycle driven by waste heat was studied by Wang et al [13]. Optimization of the thermal parameters was done using genetic algorithm and optimized exergy efficiency was 43% for a given condition. Although research has been carried out in the combined power and cooling cycles, no attempt has been made on the GAX based combined systems. In this paper, the thermodynamic analysis of the GAX based absorption power and cooling cycle is presented.

Working Principle

The schematic of a simple absorption power and cooling cycle is shown in Figure 1.

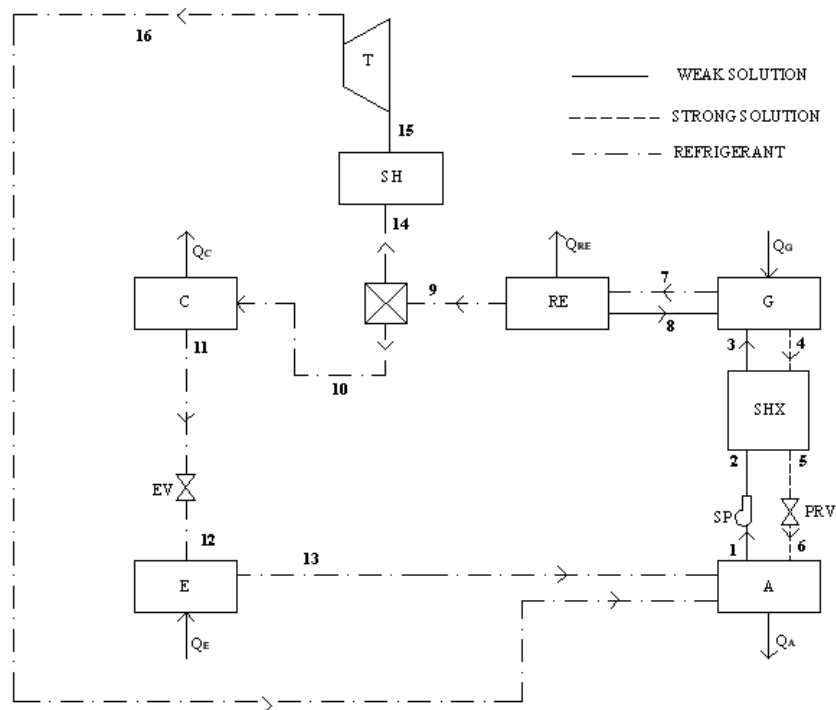


Figure 1: Schematic of a simple absorption power and cooling cycle

Weak solution from the absorber is pumped by a solution pump (SP) to the generator through a solution heat exchanger (SHX). The weak solution is heated by an external heat source in the generator (G) which drives off the refrigerant vapor. The refrigerant vapour from the generator enters the rectifier (RE) for purification. The purified refrigerant vapour from the rectifier is split into two portions by a split ratio (S). Split ratio is defined as the ratio of the refrigerant mass flow rate that enters the condenser (C) to the total refrigerant mass flow rate in the cycle. One portion of the refrigerant vapour after getting condensed in the condenser, is then throttled in the expansion valve (EV) before it produces the cooling effect in the evaporator (E). The remaining portion of the refrigerant vapour from the rectifier enters the super heater (SH). The super heated refrigerant vapour after expansion in the turbine (T) to generate power enters the absorber. The strong solution returns from the generator to the absorber through the solution heat exchanger and a pressure reducing valve (PRV).

Pinch Point approach is used in the analysis to recover the internal heat present in the various stream of solutions, refrigerant liquid as well as vapour in order to reduce the generator heat input. HPHAX, LPGAX, Solution cooler are incorporated to achieve the same. The cycle is modified and Figure 2 shows the schematic of a GAX based absorption power and cooling cycle. The weak solution is pumped by a solution pump from the absorber into the high pressure GAX (HPGAX). The HPGAX eliminates the necessity of a separate rectification column in this system. The HPGAX cools the refrigerant vapour (state point 13) coming from the generator through the solution cooler (SC), by the incoming weak solution (state point 2). As a result of the heat and mass transfer between the refrigerant vapour and the weak solution, the temperature of the refrigerant vapour reduces and its ammonia mass fraction increases, and at the same time the system performance is enhanced due to the reduction in the thermal energy in the generator.

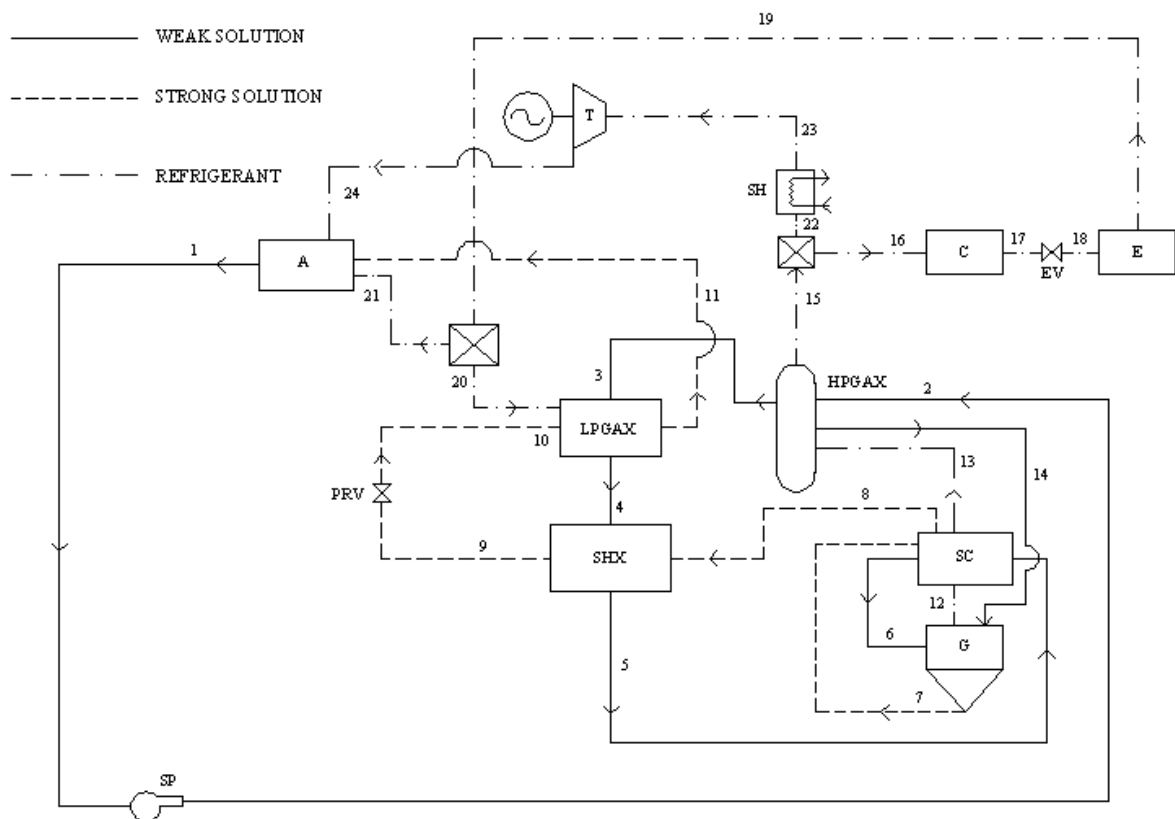


Figure 2: Schematic of a GAX based absorption power and cooling cycle

The heated weak solution enters the low pressure GAX (LPGAX) (state point 3). In the LPGAX, the strong solution (state point 10) returning from the generator (state point 7) through the solution heat exchanger (SHX) is cooled by the incoming weak solution (state point 3), while absorbing a partial amount of the low pressure refrigerant vapour (state point 20) from the evaporator. The strong solution, after partial absorption of the refrigerant vapour in the LPGAX (state point 11), enters the absorber for complete absorption and becomes strong in refrigerant. Then, the weak solution enters the SHX (state point 4), where it exchanges heat with the strong solution (state point 8). The weak solution finally enters the generator (state point 6) through the SC (state point 5), where it gets heated up further by the strong solution leaving the generator (state point 7). In the generator, the refrigerant is boiled out from the weak solution and the refrigerant vapour enters the HPGAX (state point 13) through SC (state point 12). The enriched refrigerant vapour from the HPGAX (state point 15) is split into two portions. One portion of the refrigerant vapour after getting condensed in the condenser (state point 17) is throttled in the expansion valve before it produces the cooling effect in the evaporator. The remaining portion of the refrigerant vapour (state point 22) from the HPGAX enters the super heater. The super heated refrigerant vapour (state point 23) after expansion in the turbine to generate power enters the absorber (state point 24) to complete the cycle.

Simulation study

The following assumptions were made to conduct simulation studies to evaluate the performance of the GAX based absorption power and cooling cycle.

1. The system operates under a steady state condition.
2. The frictional pressure drop in the cycle is neglected except through the expansion device.
3. The weak solution leaving the absorber (state point 1) and the strong solution (state point 7) leaving the generator are saturated.
4. The concentration of the refrigerant leaving the HPGAX is 0.999 (state point 15).
5. The refrigerant leaving the condenser (state point 17) and evaporator is saturated (state points 19).
6. Pump work is neglected.
7. The effectiveness of SHX and the temperature of super heater are assumed to be 0.75 and 450K, respectively.
8. The weak solution entering the solution cooler (state point 5) is at minimum generator temperature.
9. The refrigerant vapour leaving the SC at state point 13 is in equilibrium with the weak solution at state point 5.
10. Split factor (Z) is taken to be 0.8. (Split factor is defined as the ratio of the mass flow rate of the refrigerant to the absorber to the mass flow rate of the refrigerant from the evaporator).

The correlations for determining the thermodynamic properties at various state points are referred from Sun [14,15]. The input parameters of the simulation program are the temperatures of the absorber (t_A), condenser (t_C), evaporator (t_E), generator (t_G), the mass flow rate of the weak solution (\dot{m}_{ws}), concentration of the refrigerant vapour leaving the HPGAX (X_{15}), split ratio (S) and the effectiveness of the SHX. For a given set of input parameters, the simulation program determines the cooling capacity, power output, COP, thermal efficiency and also the heat load at each component of the cycle, under different operating conditions.

The equations that were used in the performance analysis are as follows.

$$Q_A = m_{11} h_{11} + m_{21} h_{21} + m_{24} h_{24} - m_1 h_1 \quad (1)$$

$$Q_C = m_{16}(h_{16} - h_{17}) \quad (2)$$

$$Q_E = m_{18}(h_{19} - h_{18}) \quad (3)$$

$$Q_G = m_7 h_7 + m_{12} h_{12} - m_6 h_6 - m_{14} h_{14} \quad (4)$$

$$Q_{HPGAX} = m_{ws}(h_3 - h_2) \quad (5)$$

$$Q_{LPGAX} = m_{ws}(h_4 - h_3) \quad (6)$$

$$Q_{SHX} = m_{ws}(h_5 - h_4) \quad (7)$$

$$Q_{SC} = m_{ss}(h_7 - h_6) \quad (8)$$

$$Q_{SH} = m_{22}(h_{23} - h_{22}) \quad (9)$$

$$P = m_{23}(h_{23} - h_{24}) \quad (10)$$

The coefficient of performance is the ratio of the evaporator heat load to the generator heat input.

$$COP = \frac{Q_E}{Q_G} \quad (11)$$

Thermal Efficiency (η) is defined as the ratio of the sum of the cooling effect and the power output to the sum of the generator heat input and the super heater heat input.

$$\eta = \frac{(Q_E + P)}{(Q_G + Q_{SH})} \quad (12)$$

Results and Discussion

The simulation studies on the GAX based absorption power and cooling cycle is performed for generator temperatures varying between 120°C and 160°C in steps of 10°C. The sink temperature is varied between 25°C and 45°C in steps of 5°C and the evaporator temperature is varied between -10°C and 10°C in steps of 5°C. The split ratio is varied between 0 and 1 in steps of 0.2.

The variation of the cooling capacity, power output, COP and thermal efficiency of both the simple and the GAX cycles, with respect to the generator temperatures, for a constant sink temperature and split ratio, is shown in Figure 3. Referring to Figure 3a and 3b, at a constant evaporator temperature, as the generator temperature increases, the decrease in the strong solution concentration increases the degassing width. The increase in the degassing width decreases the circulation ratio. The decrease in the circulation ratio increases the refrigerant mass flow rate, since the weak solution mass flow rate is constant. Hence, the cooling capacity and the power output increases. Since the cooling capacity and the power output remains the same for both the cycles, they are represented by same lines. At a constant generator temperature, as the evaporator temperature is increased from -10°C to 10°C, the circulation ratio is still lower and the refrigerant mass flow rate is higher. Therefore, the cooling capacity and the power output is higher at $t_E = 10^\circ\text{C}$. Referring to Figure 3c and 3d, the solid and dashed lines represent the simple and GAX cycles respectively. The COP and the thermal efficiency of the simple cycle remains almost constant at $t_E = -10^\circ\text{C}$ and decreases marginally at $t_E = 10^\circ\text{C}$, and that of the GAX cycle decreases marginally, at both the evaporating temperatures This is

due to the increase in the generator heat load which is more significant than the increase in the evaporator heat load.

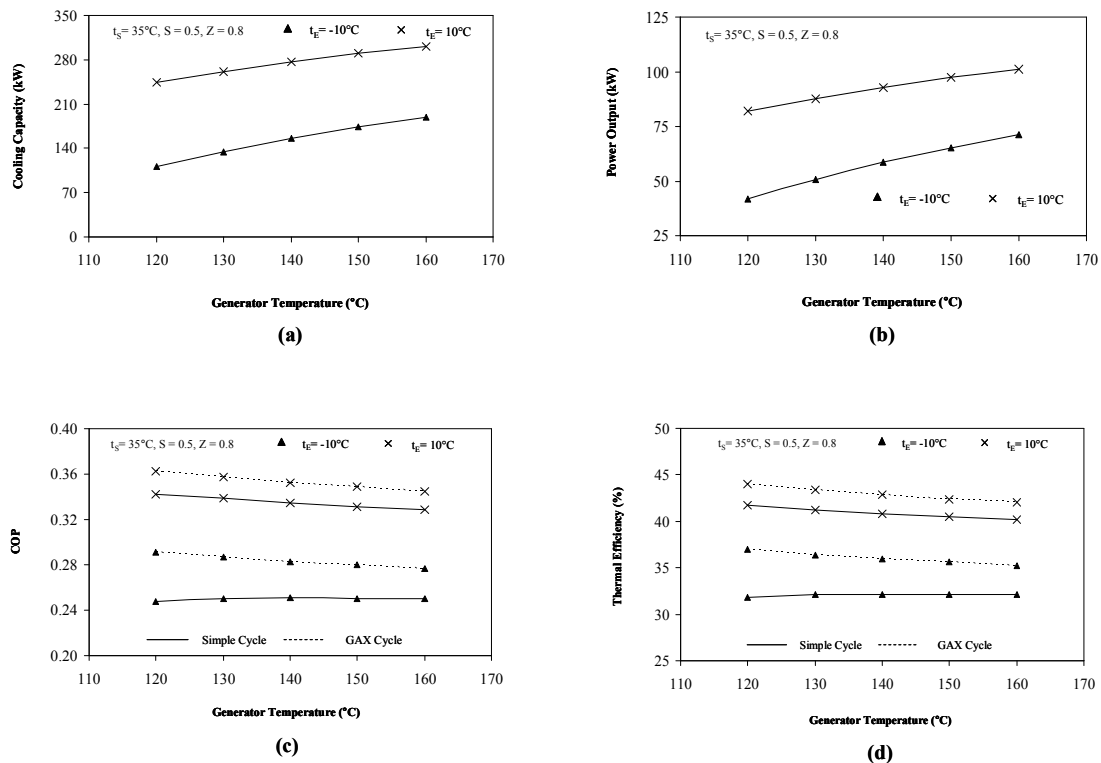


Figure 3: Variation of the cooling capacity, power output, COP and thermal efficiency with the generator temperatures

At a constant generator temperature, the COP and the thermal efficiency of the GAX cycle is higher than that of the simple cycle. This is due to the decrease in the absorber heat load and subsequently the generator heat load because of reduction in the mass flow rate of the refrigerant vapour being absorbed in the absorber in the GAX cycle.

Figure 4 depicts the variation of the cooling capacity, power output, COP and thermal efficiency of both the simple and the GAX cycles, with the sink temperatures. The evaporator temperature is maintained constant at 0°C . With an increase in the sink temperature, the concentration of the weak and strong solution decreases and increases respectively, at a constant generator temperature. Due to this, the degassing width decreases and it results in increase in the circulation ratio. For a constant weak solution mass flow rate, the increase in the circulation ratio reduces the refrigerant mass flow rate. Hence, the cooling capacity and the power output decreases. When the generator temperature is increased from 120°C to 160°C , the degassing width increases and it decreases the circulation ratio. The reduction in the circulation ratio increases the refrigerant mass flow rate, since the weak solution mass flow rate is constant. Therefore, the cooling capacity and the power output is higher at $t_g = 160^\circ\text{C}$. The cooling capacity and the power output of both the cycles are represented by the same lines (Figure 4a and 4b), since it remains same for both the cycles at a fixed sink temperature. The COP of both the cycles decreases as inferred from the Figure 4c, due to reduction in the cooling capacity and increase in the generator heat load because of higher mass flow rate of the strong solution at higher sink temperatures. Similarly, the thermal efficiency of both the cycles decreases (Figure 4d). The COP and the thermal efficiency of the GAX cycle is higher when

compared to that of the simple cycle, for the same operating conditions, due to the reduction in the mass flow rate of the refrigerant vapour being absorbed in the absorber in the GAX cycle.

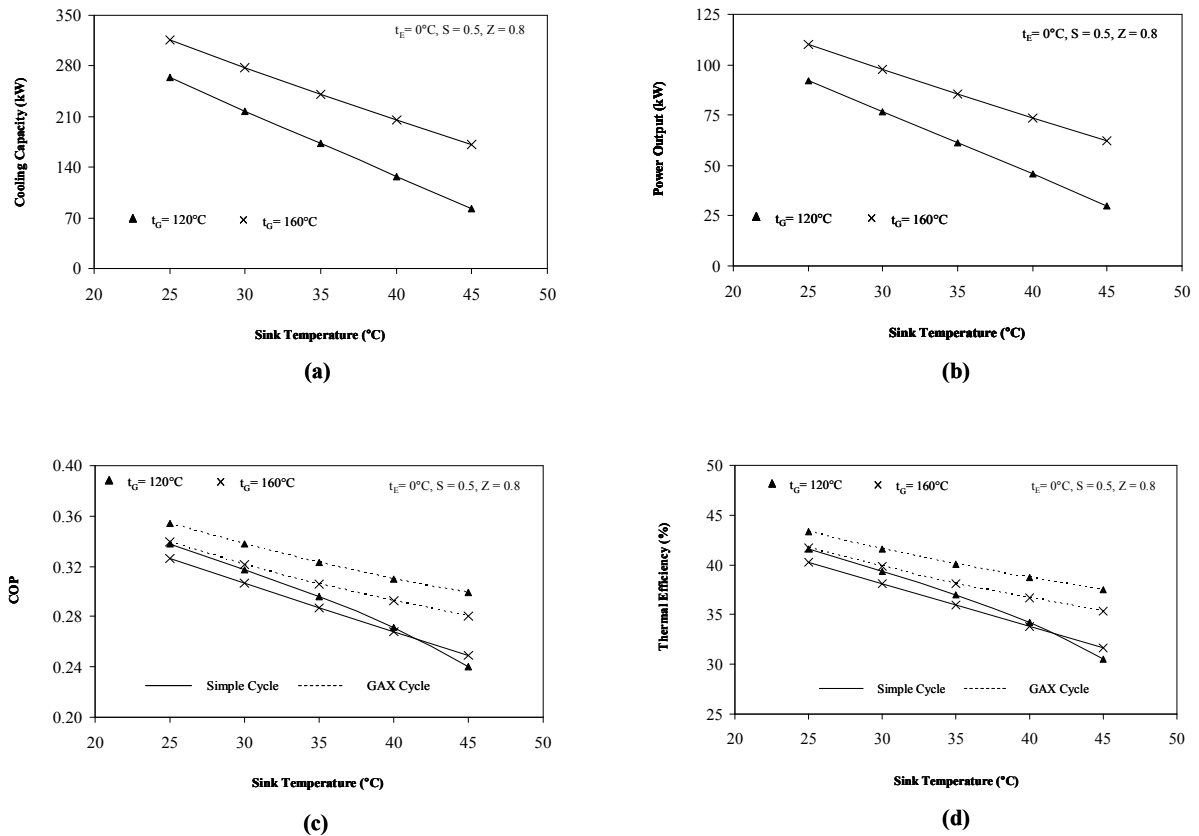


Figure 4: Variation of the cooling capacity, power output, COP and thermal efficiency with the sink temperatures

The variation of the cooling capacity, power output, COP and thermal efficiency of both the simple and the GAX cycles, with respect to the evaporator temperatures, at a constant generator temperature is shown in Figure 5.

With an increase in the evaporator temperature, the degassing width increases, due to increase in the concentration of weak solution, at a constant sink temperature. Because of this, the circulation ratio decreases and it increases the refrigerant mass flow rate. Therefore, the cooling capacity and the power output increases as inferred from Figure 5a and 5b, respectively. When the sink temperature is increased from 25°C to 45°C , at a constant evaporator temperature, the degassing width decreases and it increases the circulation ratio. Due to this, the refrigerant mass flow rate decreases and hence the cooling capacity and the power output is lower at $t_s = 45^\circ\text{C}$. From the Figure 5c and 5d, it is observed that the COP and the thermal efficiency of both the cycles increases respectively, with respect to evaporator temperatures, due to increase in the cooling capacity, which is more significant than the increase in the generator heat load. As explained in the earlier section, the COP and thermal efficiency of the GAX cycle is higher than that of the simple cycle for the same operating conditions.

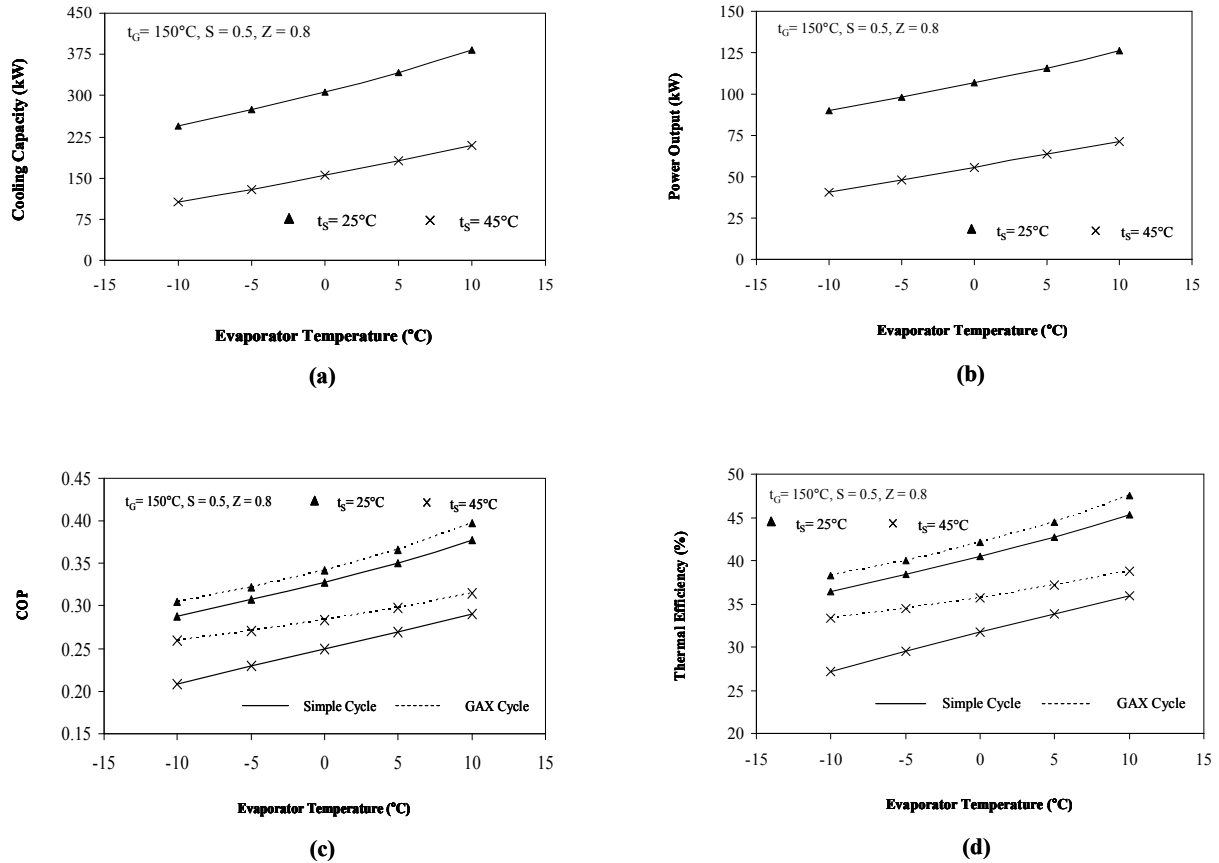


Figure 5: Variation of the cooling capacity, power output, COP and thermal efficiency with the evaporator temperatures

Figure 6 shows the variation of the cooling capacity and the power output with the split ratio for constant generator and sink temperatures of 150°C and 35°C respectively. The evaporator temperature is varied between -10°C and 10°C. At a constant evaporator temperature, as the split factor increases, the increase in the refrigerant mass flow to the cooling part and decrease in the refrigerant mass flow rate to the power part, increases and decreases the cooling capacity and the power output respectively, of both the simple and GAX cycles. As discussed in the earlier section, when the evaporator temperature is increased, the cooling capacity and the power output of both the cycles increases. It is inferred from the

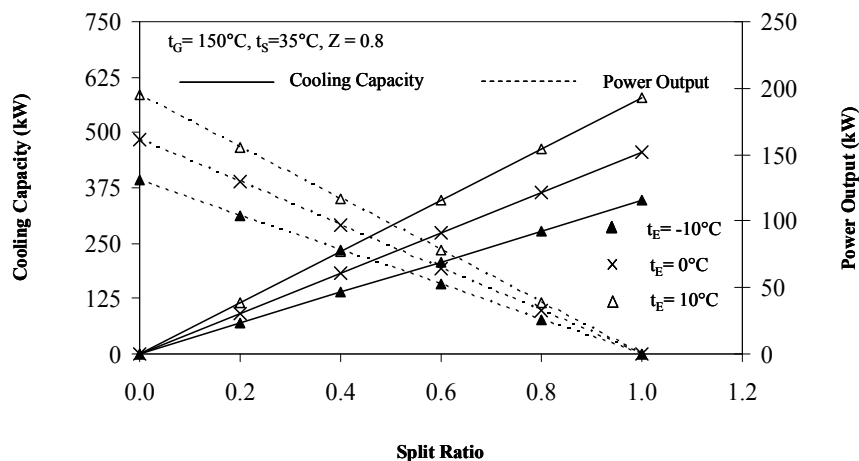


Figure 6: Variation of the cooling capacity and the power output with the split ratio

Figure that, between split ratio 0.4 and 0.6, both the solid and the dotted lines intersect. Hence the optimum split ratio is taken to be 0.5. At the optimum split ratio, the cooling capacity and the power output of both the cycles are 225 kW and 80 kW respectively, corresponding to an evaporator temperature of 0°C.

The variation of the performance of the cooling cycle and the combined cycle with respect to the split ratio is depicted in Figure 7. The generator, sink and evaporator temperatures are kept constant at 150°C, 35°C and -10°C respectively. With an increase in the split ratio, the increase in the cooling capacity increases the COP of both the cycles. The COP of the simple and GAX cycle reached a maximum of 0.50 and 0.63 respectively, for the operating conditions shown in the Figure. Similarly, the thermal efficiency of both the cycles increases due to the increase in

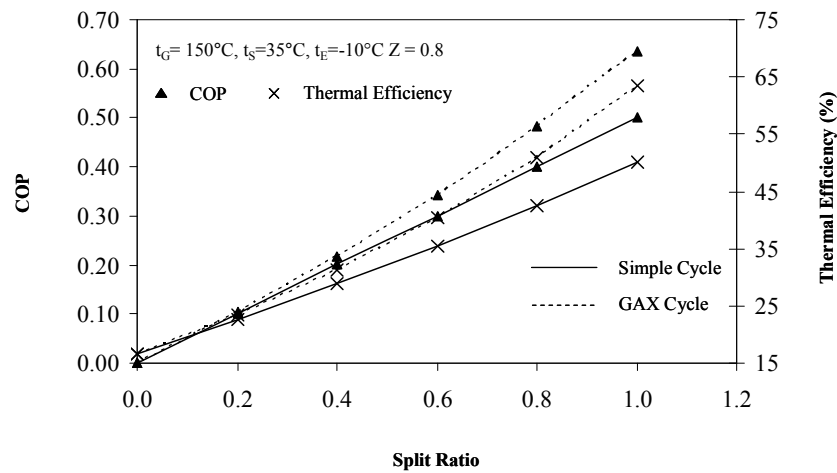


Figure 7: Variation of the COP and the thermal efficiency with the split ratio

the performance of the cooling part of the cycle. The thermal efficiency reached a maximum of about 50% for the simple cycle, while for the GAX cycle it is about 64%. Figure 8 depicts the variation of the internal heat recovered and the thermal efficiency of both the cycles, with the generator temperatures, for constant sink and evaporator temperatures of 35°C and

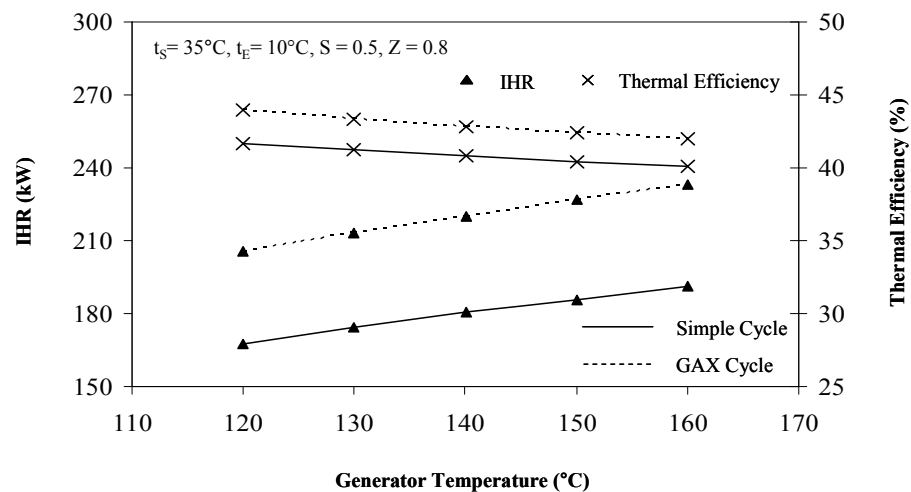


Figure 8: Variation of the internal heat recovered and the thermal efficiency with the generator temperatures

10°C, respectively. The internal heat recovered in the simple cycle is the amount of heat recovered in the solution heat exchanger (SHX). As the generator temperature increases, the amount of heat recovered by the weak solution from the strong solution increases in SHX. Due to this, heat load of the SHX increases. In the GAX cycle, the internal heat recovered is the summation of the heat load of the heat recovery components such as HPGAX, LPGAX, SHX and SC. With increase in the generator temperature, the refrigerant mass flow rate increases. Therefore, the heat gained by the weak solution in the HPGAX and the LPGAX increases. Similar to SHX in the simple cycle, the heat load of the SC in the GAX cycle also increases and hence the total amount of internal heat recovered increases.

Conclusion

Thermodynamic analysis of the GAX based absorption power and cooling cycle has been carried out for different generator, sink, evaporator temperatures and split ratio. The split ratio has been optimized and the optimum value was found to be 0.5. At the optimum split ratio, for constant generator, sink and evaporator temperatures of 150°C, 35°C and 0°C respectively, the cooling capacity and the power output of both the cycles were 225 kW and 80 kW respectively. The COP and the thermal efficiency of the GAX based cycle was found to be higher than that of the simple cycle for the various operating conditions analyzed.

Nomenclature

h	specific enthalpy [kJ kg^{-1}]
\dot{m}	mass flow rate [kg s^{-1}]
p	pressure [kPa]
P	power output [kW]
Q	heat load [kW]
S	split ratio
t	temperature [$^{\circ}\text{C}$]
T	temperature [K]
X	ammonia mass fraction
Z	split factor

Subscripts

A	absorber
C	condenser
E	evaporator
G	generator
r	refrigerant
S	sink
ss	strong solution (strong in absorbent, weak in refrigerant)
ws	weak solution (weak in absorbent, strong in refrigerant)

Abbreviations

A	absorber
C	condensor
COP	coefficient of performance
CR	circulation ratio
E	evaporator

EV	expansion valve
G	generator
GAX	generator absorber heat exchange
HPGAX	high pressure GAX
IHR	internal heat recovered
LPGAX	low pressure GAX
PGAX	GAX cycle for panel heating
PRV	pressure reducing valve
RE	rectifier
SC	solution cooler
SH	super heater
SHX	solution heat exchanger
SP	solution pump
T	turbine

References

- 1) Pouraghaie M., Atashkari K., Besarati S.M., Narimen-zadeh, N., 2010, "Thermodynamic performance optimization of a combined power/cooling cycle", Energy Conversion and Management, Vol 51, No 1, pp. 204 -211.
- 2) Kalina A.I., 1983, "Combined cycle and waste-heat power systems based on a novel thermodynamic energy cycle utilizing low-temperature heat for power generation", ASME paper: 83-JPGC-GT-3.
- 3) Marston C.H., 1990, "Parametric analysis of the Kalina cycle", Journal of Engineering Gas Turbines Power, Vol 112, No 1, pp. 107-116.
- 4) Rogdakis E.D., Antonopoulos K.A., 1991, "A high efficiency NH₃/H₂O absorption power cycle", Heat Recovery Systems and CHP, Vol 11, No 4, pp. 263-275.
- 5) Ibrahim O.M., Klein S.A., 1996, "Absorption power cycles", Energy, Vol 21, No 1, pp. 21-27.
- 6) Xu F., Goswami D.Y., Bhagwat S.S., 2000, "A combined power / cooling cycle", Energy, Vol 25, No 3, pp. 233-246.
- 7) Lu S., Goswami D.Y., 2002, "Theoretical analysis of ammonia based combined power/refrigeration cycle at low refrigeration temperatures", Proceedings of solar sunrise on the reliable energy economy, June 15-20, 2002, Reno, Nevada.
- 8) Tamm G., Goswami D.Y., Lu S., Hasan A.A., 2004, "Theoretical and experimental investigation of an ammonia-water power and refrigeration thermodynamic cycle", Solar Energy, Vol 76, No 1-3, pp. 217-228.
- 9) Zheng D., Chen B., Qi Y., Jin, H., 2006, "Thermodynamic analysis of a novel absorption power/cooling combined-cycle", Applied Energy, Vol 83, No 4, pp. 311-323.

- 10) Martin C., Goswami D.Y, 2006, “Effectiveness of cooling production with a combined power and cooling thermodynamic cycle”, *Applied Thermal Engineering*, Vol 26, No 5-6, pp. 576-582.
- 11) Liu M., Zhang N., 2007, “Proposal and analysis of a novel ammonia-water cycle for power and refrigeration cogeneration”, *Energy*, Vol 32, No 6, pp. 961-970.
- 12) Zhang N., Lior N., 2007, “Methodology for thermal design of novel combined refrigeration/power binary fluid systems”, *International Journal of Refrigeration*, Vol 30, No 6, pp. 1072-1085.
- 13) Wang J., Dai Y., Gao L., 2008, “Parametric analysis and Optimization for a combined power and refrigeration cycle”, *Applied Energy*, Vol 85, No 11, pp. 1071-1085.
- 14) Sun D.W., 1996, “Thermodynamic design data and optimum design maps for absorption refrigeration systems”, *Applied Thermal Engineering*, Vol 17, No 3, pp. 211-221.
- 15) Sun D.W., 1998, “Comparison of the performances of NH₃-H₂O, NH₃-LiNO₃ and NH₃-NaSCN absorption refrigeration systems”, *Energy Conversion and Management*, Vol 39, No 5-6, pp. 357–368.